

Instrumental determination of phosphorus in silicon for photovoltaics by β spectroscopy: a new approach

B. Karches¹ · K. Welter¹ · C. Stieghorst^{1,3} · N. Wiehl¹ · T. Reich¹ ·
S. Riepe² · P. Krenckel² · H. Gerstenberg³ · C. Plonka¹

Received: 17 June 2016 / Published online: 23 September 2016
© Akadémiai Kiadó, Budapest, Hungary 2016

Abstract In this study, we report on the investigation of a β - γ -anticoincidence set up for the determination of phosphorus in silicon for photovoltaics by Instrumental Neutron Activation Analysis. For the suppression of disturbing β/γ radiation emitted by impurities, a plastic scintillator for β -detection is surrounded by a well type NaI(Tl) γ -detector. A suppression of 40 % for the impurities ⁶⁰Co and ¹²⁴Sb could be achieved. The limit of detection was determined to be less than 0.1 ppm. In order to correct different β absorption, dedicated Geant4 simulations were used. With first quantitative measurements the phosphorus concentration in silicon could be determined.

Keywords β - γ -Anticoincidence · Instrumental β spectroscopy · Solar grade silicon · Phosphorus · Photovoltaic · INAA

Introduction

Motivation

Photovoltaics is one of the key technologies for the development of renewable energies. In this context, solar

grade silicon (SoG-Si) with a required purity of at least 99.99999 % is an important material for solar cell production. The efficiency of a solar cell is strongly influenced by dopants, e.g. phosphorus and boron. Although most of the SoG-Si is boron doped (p-type-Si), studies show the advantages of phosphorus doped silicon (n-type-Si) [1–3]. Due to this fact, the quantitative determination of the phosphorus concentration in silicon is of great interest. Most of the common methods for the analysis of phosphorus are based on wet chemistry, which normally requires dissolutions of the samples [4]. To dissolve silicon, highly toxic hydrofluoric acid is needed, and the risk of possible contaminations and incomplete conversion increases, hence an instrumental method for the determination of phosphorus in solar grade silicon would be advantageous.

In the framework of a project about the determination of impurities in SoG-Si of the University of Mainz and the Fraunhofer Institute of Solar Energy Systems (ISE), a method for the analysis of phosphorus in solar silicon was developed. As purification and crystallization process of silicon, the so called directional solidification is used at the Fraunhofer ISE. During this solidification from bottom to top, the impurities accumulate at the top due to their low segregation coefficients. The instrumental neutron activation analysis (INAA) is well-established in the instrumental determination of trace elements in solar silicon because of its accuracy and non-destructive nature. Therefore, it was chosen for the quantification of phosphorus and the determination of impurities like the 3d-transition metals in the project [5]. However, some challenges occur for the detection of phosphorus with INAA, since the only activation product ³²P is a pure β emitter. Measuring ³²P instrumentally by β spectrometry requires the elimination of β particles emitted by other isotopes in the sample. The

✉ B. Karches
karches@uni-mainz.de

¹ Institute of Nuclear Chemistry, Johannes Gutenberg-University Mainz, Fritz-Strassmann-Weg 2, 55128 Mainz, Germany

² Fraunhofer Institute for Solar Energy Systems (ISE), Heidenhofstraße 2, 79110 Freiburg, Germany

³ Heinz Maier-Leibniz Zentrum, Technical University of Munich, Heidenhofstraße 2, 79110 Freiburg, Germany

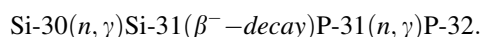
determination of phosphorus using INAA has been realized several times before, for example by shielding the disturbing β particles with acrylic glass or by varying the irradiation conditions [6–9]. Another option to reduce the disturbing β emitter is the β - γ -anticoincidence, which was already applied successfully for the detection of Sr-90 in environmental samples [10]. The β - γ -anticoincidence utilizes the fact, that β signals occurring together with a γ signal can be rejected by simultaneous detection. Thus, pure β emitters can be identified and detected almost without statistical losses. This advantage is of particular importance, because of the low phosphorus concentration at sub-ppm level. Based on these considerations, the β - γ -anticoincidence was tested for determining the phosphorus concentration in SoG-Si.

Measurement requirements and challenges

First of all, the LOD for phosphorus has to be below the expected concentration in the investigated silicon, which lies in the range of 5×10^{15} – 2×10^{15} a cm^{-3} (0.1 – $0.05 \mu\text{g g}^{-1}$). This range is of interest for the use in solar cells due to the electric material properties needed for optimum cell efficiency. Such low detection limits are in principle possible using β spectrometry.

Due to the high-purity of SoG-Si, the number of elements disturbing the determination of phosphorus is limited and no other pure β emitter is expected [5, 11]. The main impurities are cobalt, chromium, iron, manganese, antimony and boron.¹ Their β spectra and the one from the silicon matrix can overlay the ^{32}P spectrum. The produced isotopes of manganese, boron and silicon have rather short half-lives compared to ^{32}P with 14.32 days, which offers the possibility to wait until they are almost completely decayed before performing the ^{32}P measurement. In case of chromium, the only long-living radionuclide is ^{51}Cr , which decays through electron capture, thus without emitting β -particles. Consequently, the radionuclides disturbing the analysis of phosphorus are mainly ^{60}Co , ^{59}Fe , ^{124}Sb and ^{122}Sb . The emission of the β particles and the related γ quanta is almost simultaneously for these radionuclides, therefore a coincident measurement is possible.

Another detrimental effect on the measurement of phosphorus in SoG-Si is additional ^{32}P , which is generated during the irradiation of silicon by the following reaction chain:



¹ High concentrations of sulfur are also not expected, due to the measured resistivity. Although ^{32}P is an activation product of sulfur an impact on the measurement can be neglected.

This additionally generated ^{32}P has an impact on the LOD. Its concentration strongly depends on the irradiation conditions and was therefore determined by varying these.

Finally, the absorption of β -particles in the material is very important for quantitative β spectroscopy. Geant4 [12] was used to simulate the detector system in order to calculate correction factors for different sample and standard geometries.

Experimental

Anticoincidence set up and electronics

A diagram with the detector's electronic schema is provided in Fig. 1. A well-type NaI(Tl)-detector (50 mm diameter and 60 mm thickness, hole: 20 mm diameter and 40 mm length, Integral Line from Harshaw) was used for the detection of the γ rays. The β detection was carried out with a plastic scintillator² (14 mm diameter and 10 mm thickness) which fit into the well of the γ detector. The plastic scintillator was fixed with an optical gel to the photomultiplier tube R1924A from Hamamatsu. The NaI(Tl)-detector was attached to a horizontal board that could be moved along a rail-system, while the β detector was fixed. The sample was put into the well of the NaI(Tl)-detector with the plastic scintillator arranged in front of the sample. The plastic scintillator was covered by an aluminium foil to minimize losses of the scintillation light. The whole set up was covered by a black coloured lid for protection against external light sources.

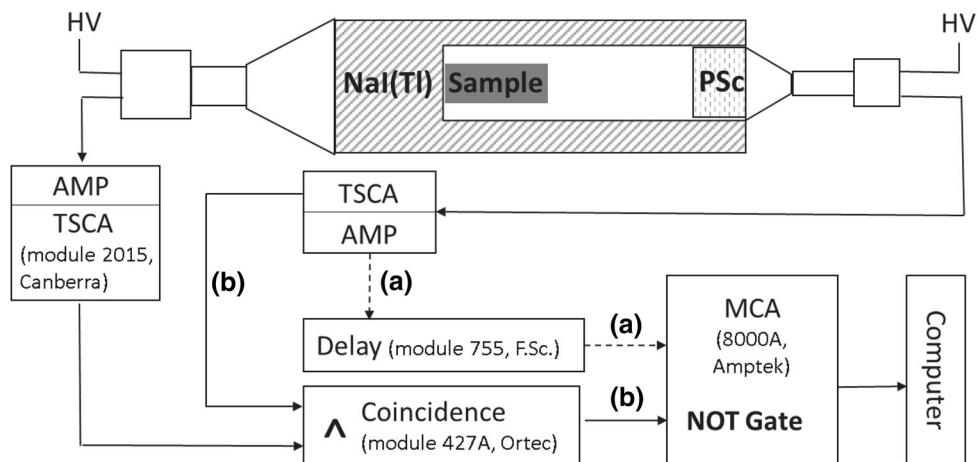
The electronic was realized by NIM-Standard modules. As coincidence unit module 755 from Philips Scientific was used and as delay amplifier module 427A from Ortec. The amplifier were Canberra 2015 modules.

A detected β signal followed two paths: (a) The signal got delayed and afterwards processed by the multichannel analyser (Pocket MCA 8000A from Amptek). The required delay time was determined by generated pulses. (b) A logic signal was created and processed by the coincidence unit. γ signals followed path b. If both signals appeared in the coincidence-module simultaneously, a signal for the NOT gate of the MCA was generated, thus discarding the β event.

The energy calibration was carried out with conversion electrons from Bi-207 and Cs-137 and β -end-point energies from ^{60}Co and ^{32}P . The efficiencies of the detectors were determined with calibrated standards of ^{32}P , ^{137}Cs and

² The plastic scintillator is of vinyltoluene, fluorescent dye is anthracene, wavelength shifter is benzimidazole- benzisochinoline-7-on (BBQ).

Fig. 1 Construction and connection scheme of the anticoincidence detector. Dashed line: way a) for β signal. PSc plastic scintillator, AMP amplifier, TSCA timing single channel analyser, MCA multi channel analyser



^{24}Na . For the plastic scintillator, the absolute efficiency is $(2.41 \pm 0.07) \%$ for ^{32}P (0–1700 keV). The peak efficiency of the NaI(Tl)-detector is $(8.76 \pm 0.01) \%$ for ^{137}Cs (662 keV) and $(6.66 \pm 0.02) \%$ for ^{24}Na (1368 keV). However, for the suppression of the disturbing radionuclides much higher percentages can be reached, because an anticoincident event can not only be detected with a γ ray from a photopeak, but also with the γ rays of the Compton continuum. Therefore, the summation of Compton continuum and photopeak is relevant for the anticoincidence measurement.

For ^{24}Na , for example, the energy range from photopeak and Compton continuum is 40–1719 keV and has a total efficiency of $(30 \pm 2) \%$. In conformance with this, a suppression of $(28 \pm 1) \%$ could be reached for ^{24}Na .

To study randomly occurring coincidences between a pure phosphorous sample and the background, a ^{32}P source (≈ 2750 Bq) was measured, giving that maximum 1 % of the events are coincident to the background. For the investigation of the accidental coincidences of γ -rays emitted by other elements such as ^{60}Co with β particles from ^{32}P , two sources of each (^{60}Co (≈ 3250 Bq), ^{32}P (≈ 2750 Bq)) were measured with a PVC shielding for the ^{60}Co electrons. The percentage of coincidences determined using this method is 8 %. The activities of the sources were chosen to be higher than the expected activity in solar silicon, in order to get an upper limit of random coincidences.

Simulations with Geant4

Compared to the absorption of γ rays, the β absorption is much more crucial for a precise analysis in β spectroscopy. Therefore, it is necessary to use standards with the same matrix as the sample, in this case silicon with known phosphorus concentration. However, the same geometry for standard and sample cannot always be ensured.

Especially in the case of different sample and standard thickness, differences in β absorptions are not negligible. In order to consider such differences, Monte Carlo simulations of the anticoincidence detector system were programmed with Geant4.

Before a simulation sequence, the geometrical parameters of the sample (height, thickness, length) as well as the material and the source were defined independently. For a given number of simulated decays, the number of detected β events and their energy deposition is calculated. By simulating the same amount of decays while varying the sample geometries, the ratio of the detected signals yields the differences in β absorption. Using this simulation sequence, a geometry correction factor (f_g) was calculated for non-identical geometries of standard and sample. This geometry factor equals the quotient of the number of counts in the simulated standard β spectrum (sim_{st}) divided by the number of counts in the sample spectrum (sim_{sa}), as shown in Eq. (1).

$$f_g = \frac{sim_{st}}{sim_{sa}} \tag{1}$$

The concentration of phosphorus in a sample (c_{sa}) was calculated according to formula (2), which contains the number of counts per mg of the sample (z_{sa}) and the standard (z_{st}), the blank values of the sample (b_{sa}) and the standard (b_{st}) and the phosphorus concentration of the standard (c_{st}).

$$c_{sa} = f_g c_{st} \frac{z_{sa} - b_{sa}}{z_{st} - b_{st}} \tag{2}$$

To validate the results of the simulation, especially for different sample thicknesses, a dedicated experiment was carried out: A ^{32}P solution was evaporated on several inactive silicon wafer of 200 μm thickness. Different numbers of these wafer were stacked up to different sample thicknesses and measured using the detector system. For the simulation, silicon samples with the thickness of the

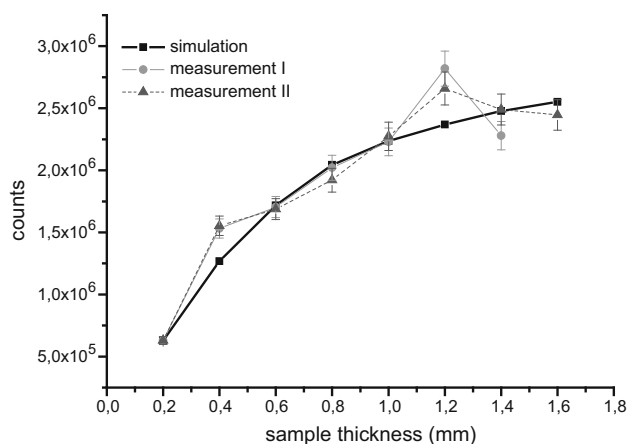


Fig. 2 Simulation and measurement of silicon samples with different thicknesses, showing a good agreement. The few outliers can be explained due to the different sizes of the manually broken samples, resulting in a lower shielding effect for some beta-particles

wafer stack and the equal number of sources were defined. The experimental data and the values given by the Geant4 simulation are in good agreement as shown in Fig. 2. This indicates, that the experiment is reproducible and furthermore that the simulation considers all relevant physical effects of the β absorption.

Experimental procedure

To investigate the effect of the anticoincidence condition on the discussed impurities, single element standards were irradiated at the research reactor TRIGA Mainz with a neutron fluence of $2.2 \times 10^{16} \text{ cm}^{-2}$ and afterwards measured using the set up with and without the anticoincidence unit. Additionally, mixtures consisting of different phosphorus to impurity ratios were measured in an analogous manner. The half-life of the sample activity was calculated based on long-term measurements and used as a tool to validate the influence of the impurity to the recorded β spectrum.

Since Sb has two different isotopes (^{122}Sb & ^{124}Sb) decaying after the irradiation, a mixture of Sb and P (5 vol% Sb/P) was measured in intervals for 45 days to differentiate between the influence of these isotopes on the measurement of phosphorous.

High-purity n-type silicon wafer ($0.7 \times 0.7 \times 0.02 \text{ cm}^3$, approx. 25 mg) with known phosphorus concentrations of $5 \times 10^{15} \text{ a cm}^{-3}$ ($0.11 \mu\text{g g}^{-1}$, Wafer 1), $9 \times 10^{14} \text{ a cm}^{-3}$ ($0.02 \mu\text{g g}^{-1}$, Wafer 2) and $5 \times 10^{14} \text{ a cm}^{-3}$ ($0.01 \mu\text{g g}^{-1}$, Wafer 3) were irradiated for the investigation of the LOD.³ Considering the phosphorous

³ The concentrations had been measured by electrical resistivity measurements.

produced by the silicon matrix during the irradiation, wafer with P concentration less than $0.001 \mu\text{g g}^{-1}$ were used as blank value. The irradiations were performed at FRM II (fluence: $6.65 \times 10^{19} \text{ cm}^{-2}$) and TRIGA Mainz (fluence: $7.3 \times 10^{17} \text{ cm}^{-2}$).

Differences in the neutron flux during the irradiations were controlled by using flux monitors. In case of the FRM II, an evaporated iron standard was used. At TRIGA Mainz the neutron flux was controlled by arranging silicon samples with known phosphorus concentration in front of and behind the samples. Due to the flat sample size, no flux variation was detected for this irradiation.

The error calculation is based on the Poisson statistic. The Gaussian error propagation was used, with the square route of the counts as absolute error for the measured counts.

Results of preliminary tests

Suppression of β spectra for specific elements

Figure 3 shows the measured β spectra of the cobalt and antimony samples with and without applying the anticoincidence condition. The difference can be seen clearly, leading to the result that the anticoincidence condition lowers the counting rate drastically, with a rejection efficiency of $(40 \pm 2) \%$ for ^{60}Co and $(38 \pm 2) \%$ for ^{124}Sb . Although the efficiency for photopeaks in the γ detector is 8 %, this suppression level can be reached, because of the contribution of the detected Compton continuum, as mentioned before. The influence of the Compton continuum is also the reason for the similar suppression of ^{60}Co and ^{124}Sb : although the photopeaks of ^{60}Co have higher γ energies and therefore are detected with less efficiency, the sum of photopeak and Compton continuum is detected with similar efficiencies for both.

For mixtures of up to 5 vol% cobalt or antimony to phosphorus, the half-life determined under anticoincidence conditions was consistent with the value for the ^{32}P half-life reported in the literature (14.32 days). Hence, if this ratio is not exceeded in a SoG-Si sample, the quantitative measurement of phosphorous is possible.

For ^{59}Fe no impact on the spectrum of ^{32}P was detected, even though the concentration used for the measurements was much higher than the expected iron concentration in SoG-Si. The reason for this is the low isotopic abundance and the low cross section of ^{58}Fe . The generated activity is very low compared to ^{32}P and is therefore negligible for the phosphorus determination employing this method.

Contrary to ^{59}Fe , ^{124}Sb strongly influences the measurement, as shown in Fig. 4. However, the long-term measurement of the Sb/P mixture indicates that 19 days

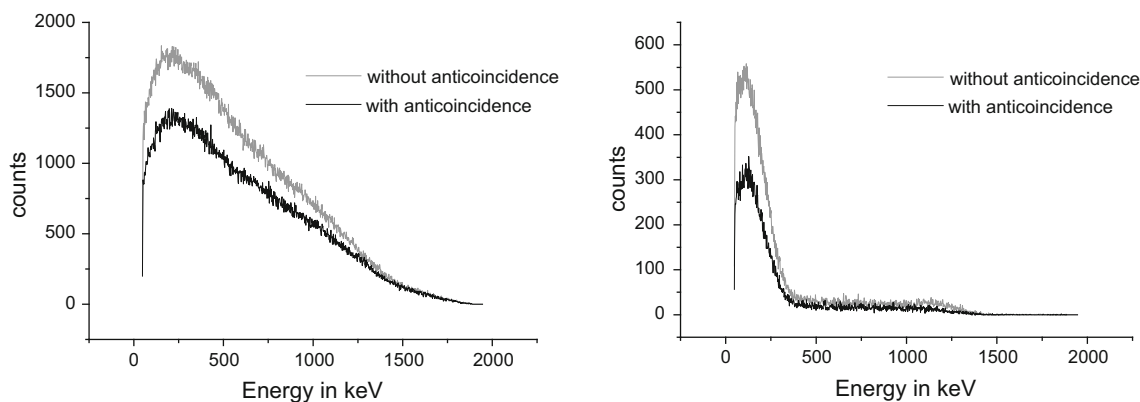


Fig. 3 β spectra of antimony (left) and cobalt (right) with and without anticoincidence

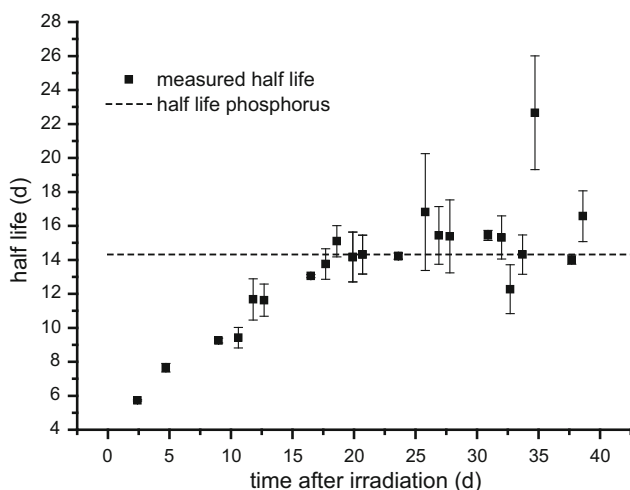


Fig. 4 Measured half-life in an activated Sb/P mixture up to 40 days after irradiation. 19–23 days after irradiation the measured half-life is conform to the literature value of ^{32}P . The unequal sizes of the error bars are due to different amounts of data taken into account

after the irradiation no impact of ^{122}Sb on the half-life can be seen, which appears as an optimal decay time for the measurements.

The results of the preliminary tests are summarized in Table 1.

Limit of detection

The counts of the measured β spectra are composed of four parts: a the counts from ^{32}P , which are of interest, b the background from the laboratory and environment, c the blank value produced during irradiation along the reaction chain (p. 4) and d the counts from disturbing radionuclides as long as the suppression is not 100 %. The Counts b–d influences the LOD, therefore they are discussed in the following.

The background was measured nine times and the average (2293 ± 16 counts h^{-1}) was used for correction.

To investigate the blank value, a quantitative estimation and two experiments (described in the experimental procedure) were performed.

With equations, which can be found elsewhere [5, 13], the blank value was estimated to be 5×10^{15} a cm^{-3} ($0.11 \mu\text{g g}^{-1}$) under the used irradiation conditions at FRM II. For the irradiation at TRIGA Mainz, a blank value of 5×10^{13} a cm^{-3} ($0.0012 \mu\text{g g}^{-1}$) was calculated.

To proof these estimations and the influence of the blank value, silicon wafer with different phosphorus concentrations were irradiated applying the two research reactors. The experimental procedure was described before. Fig. 5 shows the measured counts for three wafers with different phosphorus concentrations irradiated at FRM II after subtracting the background and normalization to 1 mg. The blank value ($b = 772.24 \pm 31.6 \text{ c}^*\text{h}^{-1}\text{mg}^{-1}$) is almost within the error range of the specific counts⁴ ($725.53 \pm 47.4 \text{ c}^*\text{h}^{-1}\text{mg}^{-1}$) resulting from Wafer 1 with a P concentration of 5×10^{15} a cm^{-3} ($0.11 \mu\text{g g}^{-1}$). This is in conformance with the calculation. Thus, the specific counts for all of the samples are lower than the blank value, which results in high uncertainties at low concentration levels. For example, the specific counts for Wafer 2 ($275.95 \pm 42.9 \text{ c}^*\text{h}^{-1}\text{mg}^{-1}$) with a P concentration of 10^{15} a cm^{-3} ($0.02 \mu\text{g g}^{-1}$) has an uncertainty of 16 %.

According to this and regarding the terms of irradiation, concentrations of phosphorus above 5×10^{15} a cm^{-3} ($0.1 \mu\text{g g}^{-1}$) can be measured with uncertainties below 10 %.

In terms of the irradiation conditions at TRIGA Mainz, no blank value was detected. But due to the lower activation, even the counts of ^{32}P from the wafer with 5×10^{15} a cm^{-3} did not exceed the background.

⁴ In this connection the term specific counts is used for the measured counts subtracted by the background and the blank value and normalized to 1 mg.

Table 1 Important radionuclides in SoG-Si, the rejection efficiency under anticoincidence and their effect on the measurement of phosphorus

Radionuclide	Rejection efficiency (%)	Effect on phosphorus measurement
^{60}Co	40	Max. 5 vol% Co/P
^{124}Sb	38	Max. 5 vol% Sb/P
^{59}Fe	–	Negligible due to low activity (up to 50 vol% Fe/P)
^{122}Sb	–	Negligible after 19 days (up to 5 vol% Sb/P)

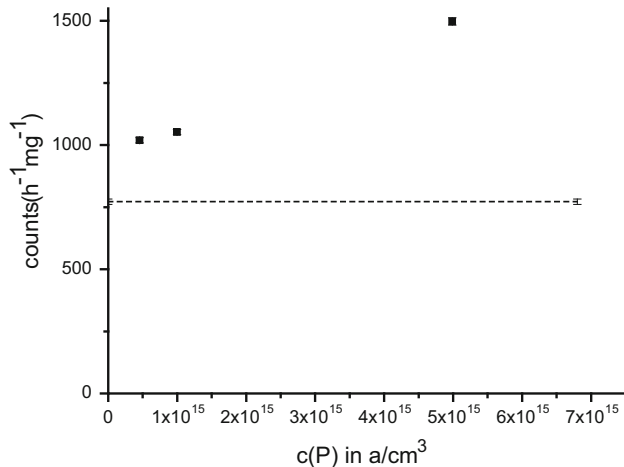


Fig. 5 Solid squares: Blank value and background corrected counts from wafer with different concentrations of phosphorus. Dashed line: blank value

Using these values, an estimation of the LOD, calculated with DIN 32645 ($\text{LOD} = 3 * \sqrt{b}$) results in $5 \times 10^{14} \text{ a cm}^{-3}$ ($0.012 \mu\text{g g}^{-1}$). However, it has to be considered that this calculation is only valid, if the suppression level of the disturbing radionuclides is 100 %. As discussed before, an influence can be seen if the Co/P ratio exceeds 5 %. This is probable at a P concentration of only $5 \times 10^{14} \text{ a cm}^{-3}$.

Quantification of phosphorus in real silicon samples

For the first quantitative determination, three multicrystalline silicon samples (I, II, III) from ingots produced at Fraunhofer ISE using the directional solidification method were analyzed. Preliminary to every solidification run of the silicon productions, the final phosphorus and boron concentrations in the silicon ingots were estimated by Fraunhofer ISE.⁵ Applying prompt gamma activation

⁵ The calculation is based on the Scheil equation [14], which describes the distribution of impurities during directional solidification. It is assumed, that the added phosphorus or boron doped silicon dissolves completely.

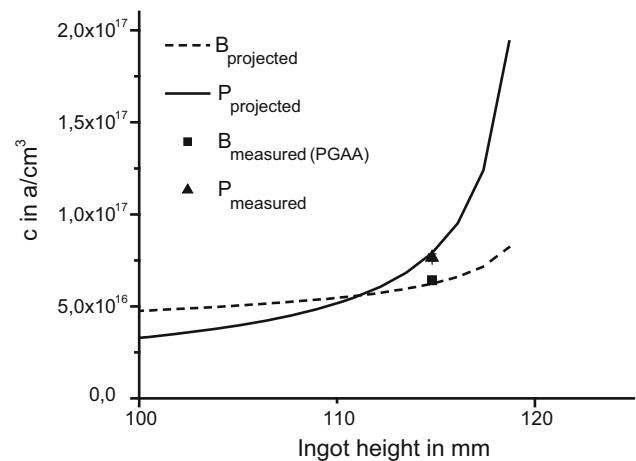


Fig. 6 Projected and measured concentrations of boron and phosphorus in a SoG-Si-ingot. The determination of phosphorus was done at TRIGA Mainz, boron was detected by PGAA at FRM II

analysis [15, 16], the upper part (approx. 50–120 mm ingot height) of the projected curve could be validated, whereas the actual boron concentration in the lower part differs from the preliminary projection [17]. One data point is exemplarily shown in Fig. 6, the whole curve can be found elsewhere [17]. Since the calculations for boron and phosphorus differ only slightly, the projected data can be used as a validation tool for high phosphorus concentration which exists at the top of the ingot. Due to that, the samples I and III were chosen from the ingot top and because their impurities concentrations do not exceed 5 vol% (element concentrations measured by γ -spectroscopy) [5].

Sample II was chosen from the bottom of the ingot to proof the method also for lower P concentrations. For the validation of this value, measurements of the resistivity could be used. At the bottom of the analyzed ingot, the boron concentration (planned: $8 \times 10^{12} \text{ a cm}^{-3}$) is 10^3 times lower than phosphorus, therefore its influence to the electrical resistivity is at the third decimal place.⁶ Therefore, measuring the resistivity can be applied as method of analysis for phosphorus.

⁶ This is obvious due to the connection of resistivity and dopant concentration [5, 18].

Using the Geant4 simulations, a quantitative determination of the phosphorus concentration was possible for all three SoG-Si samples.

Sample I ($1 \times 0.5 \times 0.5 \text{ cm}^3$, Ingot height 115 mm) was irradiated at TRIGA Mainz under the same conditions as the silicon wafer as described in the experimental section. High-purity silicon samples ($1 \times 1 \times 0.2 \text{ cm}^3$) with phosphorous concentrations of $2 \times 10^{16} \text{ a cm}^{-3}$ ($0.4 \mu\text{g g}^{-1}$) and $1 \times 10^{16} \text{ a cm}^{-3}$ ($0.2 \mu\text{g g}^{-1}$) were used as standards.

The measured and projected phosphorus concentrations in sample I are also in good agreement to each other, as pictured in Fig. 6. This demonstrates that phosphorus can be measured by applying the coincidence method at TRIGA Mainz.

The samples II and III ($1.5 \times 1 \times 0.5 \text{ cm}^3$, Ingot height 3 and 110 mm) were produced during the same directional solidification run and irradiated together at FRM II. Silicon wafers were used as standards.

In Fig. 7 and Table 2 the projected curve and the measured values of the samples are shown. The measured concentration in sample III (110 mm ingot height) is in very good agreement with the projected data. For sample II (3 mm ingot height) the measured phosphorus concentration is slightly lower than the projection, similar to the results for boron. For validation, the calculated values from the resistivity are shown in Table 2. It is obvious that they confirm the measured phosphorus concentration.

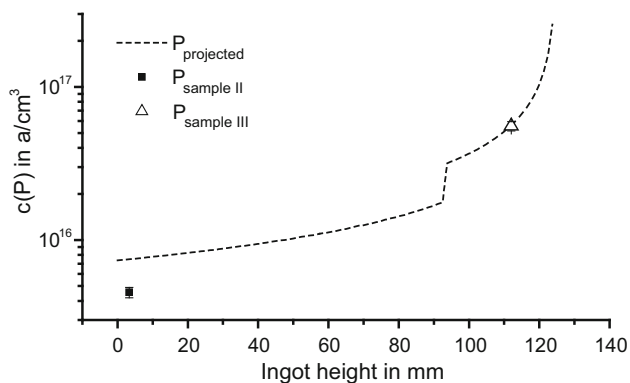


Fig. 7 Projected and measured concentration of phosphorus in a SoG-Si ingot irradiated at FRM II

Table 2 Projected, from resistivity calculated and measured phosphorus concentration in SoG-Si samples irradiated at FRM II

	Projected c(P) (a cm^{-3})	Calculated c(P) from resistance (a cm^{-3})	Measured c(P) (a cm^{-3})
Sample II	5.8×10^{16}	–	$5.6 \times 10^{16} \pm 4 \times 10^{15}$
Sample III	7.5×10^{15}	4×10^{15}	$4.6 \times 10^{15} \pm 8 \times 10^{14}$

Conclusions

In this work, a new way of measuring phosphorus concentrations in the range of ppb level in silicon for photovoltaics was presented and put into operation. This new method includes minimal sample preparation and high accuracies. The setup is based on β spectroscopy with a β - γ -anticoincidence condition to reduce possible distortions emitted by impurities. By analyzing single-element standards and mixtures of these with a phosphorus standard, the required conditions for the element composition in SoG-Si samples as well as the optimal point in time for the measurement were determined. Furthermore, the experiments show, that a LOD for this setup below $5 \times 10^{15} \text{ a cm}^{-3}$ ($0.1 \mu\text{g g}^{-1}$) is possible. The required LOD of 5×10^{15} – $2 \times 10^{15} \text{ a cm}^{-3}$ (0.1 – $0.05 \mu\text{g g}^{-1}$) for the quantification of phosphorus in SoG-Si can be reached with small improvements of the set up, e.g. a well type plastic scintillator for an increased beta detection efficiency. A simulation of the optimized geometry showed that a β detection efficiency of 30 % and a suppression level of 70 % would be possible. This would lead to a lower blank value (as estimated before for irradiations at TRIGA Mainz) and therefore to a lower LOD, since shorter irradiation times would be sufficient for measurements.

Together with prompt γ activation analysis, it is possible to determine the concentration of both dopants boron and phosphorus in the same sample by using methods of instrumental neutron activation analysis.

Acknowledgments The authors would like to thank the staff at TRIGA Mainz and FRM II for the smooth irradiations of the samples, Frank Zobel from Fraunhofer-Center for Silicon Photovoltaic (CSP) for providing several silicon samples and the Deutsche Forschungsgemeinschaft for the financial support (project no.: HA 5471/4-1 and BO 3498/1).

References

1. Ferreira, João, et al. (2010) Is n-type multicrystalline silicon the best candidate for short-term high-efficiency lower-cost solar cells? International Conference on Renewable Energies and Power Quality. <http://www.icrepq.com/icrepq'10/676-Ferreira.pdf>. Accessed 10 Sept 2016
2. Cuevas A et al (2002) Millisecond minority carrier lifetimes in n-type multicrystalline silicon. Appl Phys Lett 81(26):4952–4954
3. Cuevas A et al (2003) N-type multicrystalline silicon: a stable, high lifetime material. Proc 3rd World Conf Photovolt Energy Convers 2:1312–1315
4. Paul RL et al (2003) Radiochemical neutron activation analysis for certification of ion-implanted phosphorus in silicon. Anal Chem 75:4028–4033
5. Karches B (2016) Charakterisierung von multikristallinem solarsilicium mittels anwendungen der neutronenaktivierung. Mainz. <https://publications.ub.uni-mainz.de/theses/volltexte/2016/100000512/pdf/100000512.pdf>. Accessed 10 Sept 2016

6. Weginwar RG, Samudralwar DL, Garg AN (1989) Determination of phosphorus in biological samples by thermal neutron activation followed by beta-counting. *J Radioanal Nucl Chem* 133:317–324
7. Alfassi ZB, Lavi N (1984) Simultaneous determination of sodium, magnesium, aluminium, silicon and phosphorus by INAA using reactor and epithermal neutrons. *Analyst*. doi:[10.1039/an9840900959](https://doi.org/10.1039/an9840900959)
8. Steinnes E (1971) Determination of phosphorus in silicate rocks by neutron activation and direct beta-counting. *Anal Chim Acta* 57:451–456
9. Weckwerth G (1985) Feasibility of beta-ray spectrometry in INAA: Application in geo- and cosmochemistry. In: Sansoni B (ed) *Instrumentelle multielementanalyse*. VCH Verlag, Weinheim
10. Palazzolo RG, Samudralwar DL, Garg AN (1992) A beta spectrometer for monitoring environmental matrices. *Health Phys* 62:155–161
11. Macdonald Daniel et al (2005) Transition-metal profiles in a multicrystalline silicon ingot. *J Appl Phys* 97:033523. doi:[10.1063/1.1845584](https://doi.org/10.1063/1.1845584)
12. Agostinelli S (2003) Geant4—a simulation toolkit. *Nucl Instrum Methods Phys Res* 506:250–303
13. Seelmann-Eggebert W, Flegelheimer J, Pfennig G (1962) Die mathematische behandlung der zerfalls- und bildungsgesetze der radioaktivität mit grafisch gelösten beispielen. *Kernforschungszentrum, Karlsruhe*
14. Scheil E (1942) Bemerkung zur Schichtkristallbildung. *Z für Metallkunde* 34:70–72
15. Kudejova P et al (2008) The new PGAA and PGAI facility at the research reactor FRM II in Garching near Munich. *J Radioanal Nucl Chem* 278:691. doi:[10.1007/s10967-008-1506-9](https://doi.org/10.1007/s10967-008-1506-9)
16. Revay Z (2015) PGAA: prompt gamma and in-beam neutron activation analysis facility. *J Larg-Scale Res Facil* 1:20. doi:[10.17815/jlsrf-1-46](https://doi.org/10.17815/jlsrf-1-46)
17. Stieghorst C (2016) *Neutronenaktivierungsanalyse in archäometrie und solarenergieforschung*. Mainz. <https://publications.ub.uni-mainz.de/theses/volltexte/2016/100000548/pdf/100000548.pdf>. Accessed 10 Sept 2016
18. Hook JR, Hall HE (2013) *Solid state physics*. Wiley, Weinheim